Amine Functionalized Graphitic Carbon Nitride as Sustainable, Metal-Free Catalyst for Knoevenagel Condensation

Kamlesh Kumari, Priyanka Choudhary, Devendra Sharma, and Venkata Krishnan*

School of Chemical Sciences and Advanced Materials Research Center, Indian Institute of Technology Mandi, Kamand, Mandi 175075, Himachal Pradesh, India.

Email: vkn@iitmandi.ac.in

ABSTRACT: The design and development of novel, metal-free heterogeneous catalyst for organic transformation reactions is a challenging task. Amine functionalized graphitic carbon nitride (NH_2-GCN) was prepared and used as a heterogeneous base catalyst for Knoevenagel condensation reaction. The amine functionalization leads to increased basicity due to the presence of additional -NH_2 groups. The catalytic potential of NH_2-GCN was tested for Knoevenagel condensation, which showed a good catalytic activity. The detailed optimizations of various reaction conditions such as, time, temperature, and catalyst amount were performed. All the reactions were performed under optimal conditions, as determined. Catalyst showed highest yield of 92% and only single product is formed. It also exhibits high turnover number. In addition to that, green metrics calculations were determined. To check the heterogeneous nature of the catalyst, recyclability studies were also performed. This catalyst provides a green, sustainable, and metal-free approach for Knoevenagel condensation reaction.

KEYWORDS: Heterogeneous catalysis; graphitic carbon nitride; amine-functionalization; metal-free; Knoevenagel condensation.

1. INTRODUCTION

The most difficult aspect of synthetic organic chemistry is to perform the organic reactions to produce fine chemicals using a novel, green and sustainable approach. With the ever-increasing issues involving the environment and safety, the necessity to have novel methods to perform chemical transformation reactions is also rising.[1] So, need for the development of catalytic systems which can provide a green and sustainable approach for such chemical transformations is highly needed.

α, β unsaturated carbonyl compounds have found broad applications such as in pharmaceutical industries,[2] production of fine chemicals,[3], etc., and are quite optimistic compounds obtained from the Knoevenagel condensation reaction. This reaction involves nucleophilic attack of an active methylene moiety to a carbonyl center succeeded by the elimination of water molecule, leading to the formation of α, β unsaturated carbonyl compound.[4] Traditionally, Knoevenagel condensation is conducted by using catalysts like ionic liquids,[5] ammonium salts,[6] amino acids,[7] and amines[8] in homogeneous conditions. But the homogeneous systems have many drawbacks including high temperature, catalyst separation, recovery of catalyst, and excessive use of solvents which generates waste leading to environmental pollution.[9] And seeing the wide applications of metal-free heterogeneous catalyst, developing such catalysts for the Knoevenagel condensation turn out to be an important task. This reaction is catalyzed by using a Bronsted base, which abstracts the acidic proton of active methylene compound forming carbanion. So, base-supported catalysts have attracted much attention since it activates the nucleophiles. Over the past years, catalysts having basic properties are in discussion since they work much more efficiently by converting tandem reactions into one pot.[10] Recently, researchers have investigated a variety of heterogeneous catalysts that have been successfully implied in the formation of α, β-unsaturated carbonyl compounds to produce numerous chemicals. Heterogeneous catalysts are of enormous interest, as they have many advantages, like less generation of waste, low toxicity, high chemical, and thermal stability, earth-abundant materials, increased cost efficiency, easier separation, and better recyclability.[11] Various heterogeneous catalysts like zeolites,[12] hydrotalcite,[13] metal-organic frameworks,[14] heteropoly acids,[15] carbon-based materials,[16] and mesoporous silica[17] have been employed to perform Knoevenagel condensation.

So, in search of such robust catalysts, graphitic carbon nitride being earth-abundant, chemically, and thermally stable has gained great attention towards organic transformations.[18, 19] Graphitic carbon nitride (GCN) is a 2-Dimensional conjugated polymeric material, consisting of sp^2 hybridized C and N atoms.[20, 21] It has a graphite-like layered structure, with characteristic van der Waals forces between the sheets. The C and N are present in the ratio of 3:4 and contain a small amount of hydrogen. Since GCN is a polymeric material, the surface activity can be easily modified without changing its structure and composition.[22] In addition, it is also thermally and chemically very stable as it doesn't dissolve in acid, base, and other organic solvents. Due to its unique properties, it is considered as good metal-free catalyst for organic transformation reactions. Due to the presence of N atoms in GCN, it shows Bronsted basic and Lewis basic properties.[20] This can be further increased by introducing some basic functionalities onto the surface of the GCN. So, GCN in this regard can be employed in performing various base-catalyzed reactions.

In this work, to enhance the basicity of GCN, amine functionalization of GCN was done to synthesize NH_2-GCN catalyst. Amine functionalization was successfully done by using butylamine as an amine source and confirmed using several characterization techniques. The catalytic ability of as-synthesized NH_2-GCN was tested for Knoevenagel condensation reactions. The main objective of this work is to perform Knoevenagel condensation reactions with greener reaction conditions. Various optimizations of reaction were carried out using NH_2-GCN. And it was found that the increased basicity of GCN lead to a higher yield and better TON. The optimizations were carried out in mild conditions using the minimum amount of catalyst and environmentally friendly solvents which decrease the amount of waste generated in the reaction. So, NH_2-GCN being a metal-free heterogeneous catalyst provides a relatively novel and greener approach for the Knoevenagel condensation reaction.

2. EXPERIMENTAL SECTION

2.1. Chemicals

Dicyandiamide (99.0%, Sigma Aldrich), ethanol (≥99.5%, Merck), butylamine (>99%, Tokyo Chemical Industry), $CDCl_3$ (99.80% D, Eurisotop), DMSO-d_6 (99.80% D, Eurisotop), hexane (Fischer Scientific), ethyl acetate (Merck), were purchased and used in the reaction without

any further purification. DI water (18.2 MΩ cm) was obtained from a double-stage water purifier (ELGA PURELAB Option-R7).

2.2. Materials preparation

2.2.1. Synthesis of Graphitic Carbon Nitride (GCN) Nanosheets. Graphitic carbon nitride (GCN) nanosheets were synthesized using the reported procedure with slight modifications.[18] GCN was synthesized using dicyandiamide as a precursor wherein 5 g of dicyandiamide was taken in an alumina crucible and heated in a muffle furnace at 550 ^{o}C for 4 h at a ramp-rate of 3 ^{o}C min^{-1}. Then furnace was cooled to room temperature naturally. The yellow-colored product was obtained. The obtained solid was further crushed into fine powder and was again put in the furnace for recalcination at 500 ^{o}C for 2 h at a ramp-rate of 5 ^{o}C min^{-1}. The yellow product obtained was GCN nanosheets.

2.2.2. Synthesis of Amine-Functionalized GCN (NH_2-GCN) Nanosheets. To synthesize amine-functionalized GCN, a reported method with some modifications was followed.[23] The NH_2-GCN was prepared by using butylamine as a precursor. In detail, 500 mg of GCN was taken in a beaker having 50 mL of ethanol and sonicated for 2 h to disperse the solid particles and GCN suspension was formed. After this 2 mL of butylamine was added dropwise into GCN suspension and sonication continued for 4 h. Then it was refluxed overnight. The solution obtained was further washed with DI water 4-5 times and then dried at 80 ^{o}C. The pale, yellow-colored powder obtained was NH_2-GCN nanosheets.

2.3. Catalytic ability studies

Knoevenagel condensation. The catalytic ability of as-synthesized NH_2-GCN was studied for Knoevenagel condensation. The reaction was carried out in a 10 mL RB flask with constant magnetic stirring of 400 rpm at 25 ^{o}C. For the reaction, 1 mmol of aldehyde, 1 mmol of active methylene compound, 20 mg of NH_2-GCN (catalyst), and 3 mL of ethanol was taken in RB flask and stirred at 25 ^{o}C. Precipitation of solid product confirmed the formation of the product. The product formed beyond completion was dissolved in ethyl acetate. The catalyst was removed by centrifugation and the product was recovered by evaporating ethyl acetate using a rotary evaporator. Finally, the product was refined

through column chromatography and was characterized using ^{1}H and ^{13}C NMR spectroscopic techniques (For spectra see supporting information).

2.4. Compounds characterization

2-benzylidenemalononitrile (3a)[24]. White solid, 71%; ^{1}H NMR (500 MHz, $CDCl_3$) δ (ppm) 7.91 (d, J=7.55 Hz, 2H), 7.79 (s, 1H), 7.64 (t, J=7.64 Hz, 1H), 7.55 (t, J=7.55 Hz, 1H), 7.26 (s, 1H). ^{13}C NMR (125 MHz, $CDCl_3$) δ (ppm) 159.9, 134.6, 130.8, 130.7, 129.6, 113.7, 112.5, 82.8.

2-(4-nitrobenzylidene)malononitrile (3b)[25]. Off white solid, 92%; ^{1}H NMR (500 MHz, $CDCl_3$) δ (ppm) 8.39 (d, J=8.25 Hz, 2H), 8.08 (d, J=8.25 Hz, 2H), 7.90 (s, 1H). ^{13}C NMR (125 MHz, $CDCl_3$) δ (ppm) 156.9, 150.3, 135.7, 131.3, 124.6, 112.6, 111.6, 87.4.

2-(4-cyanobenzylidene)malononitrile (3c).[26] Off white solid, 81%; ^{1}H NMR (500 MHz, $CDCl_3$) δ (ppm) 8.00 (d, J=8.25 Hz, 2H), 7.85 (s, 1H), 7.83 (d, J=2.1, 2H). ^{13}C NMR (125 MHz, $CDCl_3$) δ (ppm) 157.3, 134.2, 133.1, 130.7, 117.2, 112.7, 111.6, 86.9.

2-(4-methylbenzylidene)malononitrile (3d)[24, 27]. Light yellow solid, 52%; ^{1}H NMR (500 MHz, $CDCl_3$) δ (ppm) 7.81 (d, J=8.20 Hz, 2H), 7.73 (s, 1H), 7.34 (d, J=7.60 Hz, 2H), 2.46 (s, 3H). ^{13}C NMR (125 MHz, $CDCl_3$) δ (ppm) 159.8, 146.4, 130.9, 130.3, 128.4, 113.9, 112.8, 81.1, 21.9.

2-(4-(dimethylamino)benzylidene)malononitrile (3e)[28]. Orange solid, 48%; ^{1}H NMR (500 MHz, $CDCl_3$) δ (ppm) 7.81 (d, J=8.90 Hz, 2H), 7.46 (s, 1H), 6.69 (d, J=9.65 Hz, 2H), 3.15 (s, 6H). ^{13}C NMR (125 MHz, $CDCl_3$) δ (ppm) 158.1, 154.2, 133.8, 119.2, 115.9, 114.9, 111.5, 71.7, 40.1.

2-(2-nitrobenzylidene)malononitrile (3f)[29]. Off white solid, 87%; ^{1}H NMR (500 MHz, $CDCl_3$) δ (ppm) 8.45 (s, 1H), 8.37 (dd, J=3.40, 1.35 Hz, 1H), 7.89 (dd, J=7.55, 4.15 Hz, 1H), 7.83-7.80 (m, 2H). ^{13}C NMR (125 MHz, $CDCl_3$) δ (ppm) 158.8, 146.7, 134.9, 130.4, 126.6, 125.8, 112.2, 110.9, 88.5.

2-(3-nitrobenzylidene)malononitrile (3g)[30]. Off white solid, 86%; ^{1}H NMR (500 MHz, $CDCl_3$) δ (ppm) 8.68 (s, 1H), 8.48 (dd, J=8.25, 1.35 Hz, 1H), 8.33 (d, J=8.25 Hz, 1H), 7.93 (s, 1H),

7.81 (t, J=8.25 Hz, 1H). ^{13}C NMR (125 MHz, $CDCl_3$) δ (ppm) 157.0, 148.5, 134.8, 131.9, 130.9, 128.2, 125.5, 112.6, 111.6, 86.6.

2-ferrocylidenemalononitrile (3h). Dark purple solid, Melting point 93-95 ^oC, 87%; ^1H NMR (500 MHz, $CDCl_3$) δ (ppm) 7.72 (s, 1H), 4.98 (s, 2H), 4.85 (s, 2H), 4.33 (s, 5H). ^{13}C NMR (125 MHz, $CDCl_3$) δ (ppm) 163.1, 115.0, 114.2, 75.2, 73.9, 71.6, 71.0.

2-(naphthalen-1-ylmethylene)malononitrile (3i)[31]. Bright yellow solid, 83%; ^1H NMR (500 MHz, $CDCl_3$) δ (ppm) 8.65 (s, 1H), 8.27 (d, J=7.55 Hz, 1H), 8.11(d, J=8.25 Hz, 1H), 7.95 (d, J=8.95 Hz, 2H), 7.70-7.59 (m, 3H). ^{13}C NMR (125 MHz, $CDCl_3$) δ (ppm) 157.7, 134.9, 133.5, 131.0, 129.4, 128.5, 128.5, 127.4, 127.3, 125.3, 122.2, 113.7, 112.5, 85.1.

2-(4-chlorobenzylidene)malononitrile (3j)[32]. Light orange solid, 60%; ^1H NMR (500 MHz, $CDCl_3$) δ (ppm) 7.86 (d, J=8.90 Hz, 2H), 7.75 (s, 1H), 7.52 (d, J=8.25 Hz, 2H). ^{13}C NMR (125 MHz, $CDCl_3$) δ (ppm) 158.3, 141.1, 131.8, 130.0, 129.2, 113.4, 112.3, 83.2.

2-(4-bromobenzylidene)malononitrile (3k)[33]. Light yellow solid, 58%; ^1H NMR (500 MHz, $CDCl_3$) δ (ppm) 7.77 (d, J=8.90 Hz, 2H), 7.73 (s, 1H), 7.69 (d, J=8.95 Hz, 2H). ^{13}C NMR (125 MHz, $CDCl_3$) δ (ppm) 158.5, 133.0, 131.8, 129.9, 129.6, 113.4, 112.3, 83.3.

3. RESULTS AND DISCUSSION

Synthesis and characterizations

The nanosheets of NH_2-GCN were synthesized successfully by amine functionalization of GCN nanosheets (as shown in Scheme 1). The amine functionalization was done using butylamine as an amine source. The GCN nanosheets were dispersed in ethanol via sonication to increase the active sites. Further treatment with butylamine resulted in functionalization of -NH_2 groups on to the GCN nanosheets which in turn increases in its basicity as compared to bare GCN.

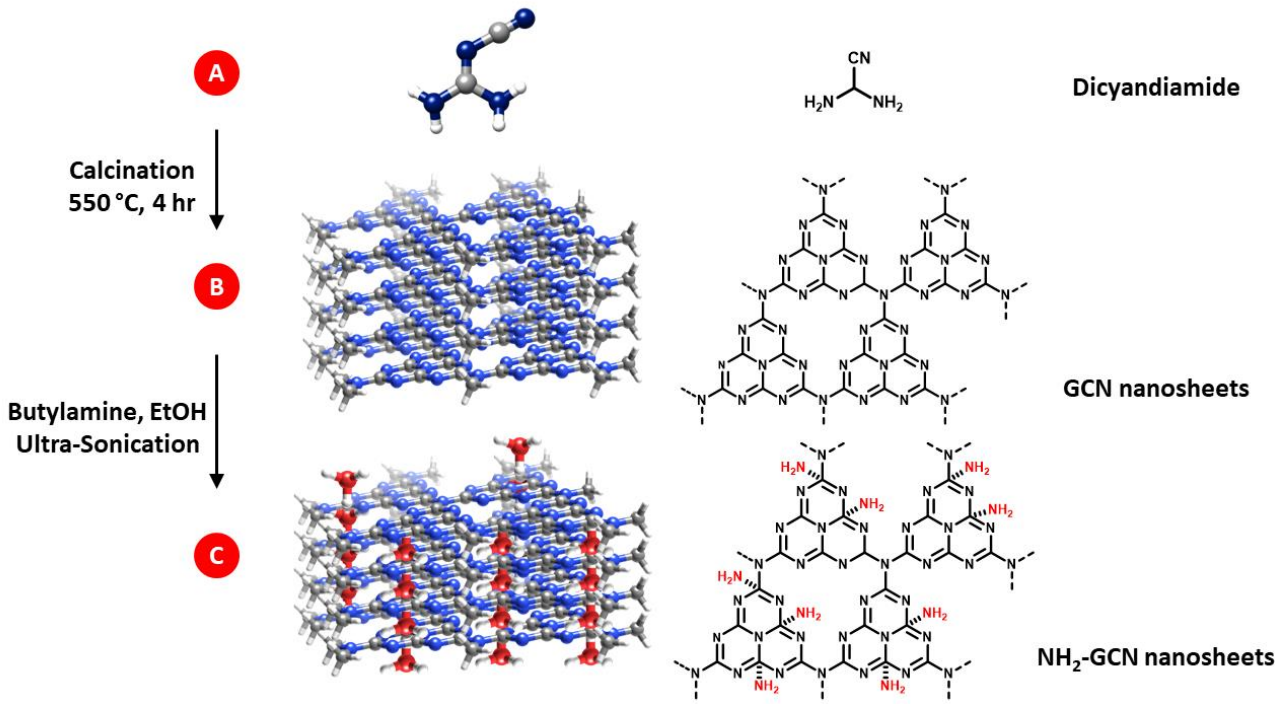

Scheme 1. Schematic representation of Synthesis of NH_2-GCN nanosheets.

Structural analysis of GCN and NH_2-GCN nanosheets was done using PXRD (powder X-ray diffraction). The PXRD patterns of GCN (Figure 1a) shows a weak angle reflection peak (100) of 13.17° which can be attributed to the inter-planar, structural packing of this motif, and a strong peak (002) at 27.62° which corresponds to characteristic carbon nitride inter-layer stacking reflection.[34] The PXRD pattern of NH_2-GCN is the same as that of GCN. After functionalization, the intensity of (100) and (002) peaks are increased as the number of $-NH_2$ groups increases. The amine-functionalized GCN shows a little variation in the (002) peak which is due to increased π-π stacking and H-bonding interactions.[35] FTIR spectra shows almost similar peaks in both GCN and NH_2-GCN catalysts. The broadband observed between 3000-3400 cm^{-1} is attributed to the N-H stretching of terminal and functionalized NH_2 groups. The breathing mode of the s-triazine ring showed a characteristic sharp peak at 806 cm^{-1}. Peaks between 1200-1400 cm^{-1} for both GCN and NH_2-GCN arises due to the C-N stretching vibrations. The peak at 1633 cm^{-1} is ascribed to C=N stretching vibrations in GCN.[36] As $-NH_2$ is already present in our material, FTIR spectroscopy cannot be employed for distinguishing between GCN and NH_2-GCN nanosheets. Furthermore, the Raman spectroscopy was used to determine molecular fingerprints of as-synthesized catalysts. The Raman spectrum was

recorded using 785 nm laser excitation source. High intensity peaks at 480 cm^{-1} and 714 cm^{-1} are attributed to the breathing modes of the heptazine ring. The peaks at 754 cm^{-1} and 979 cm^{-1} are resultant of the in-plane vibration of the C-N bond.[37] The peak at 1237 cm^{-1} arises due to the breathing modes of the triazine ring. The broadband between 1400-1800 cm^{-1} is indicative of the sp^2 and sp^3 hybridized carbons present in both GCN and NH_2-GCN.[38]

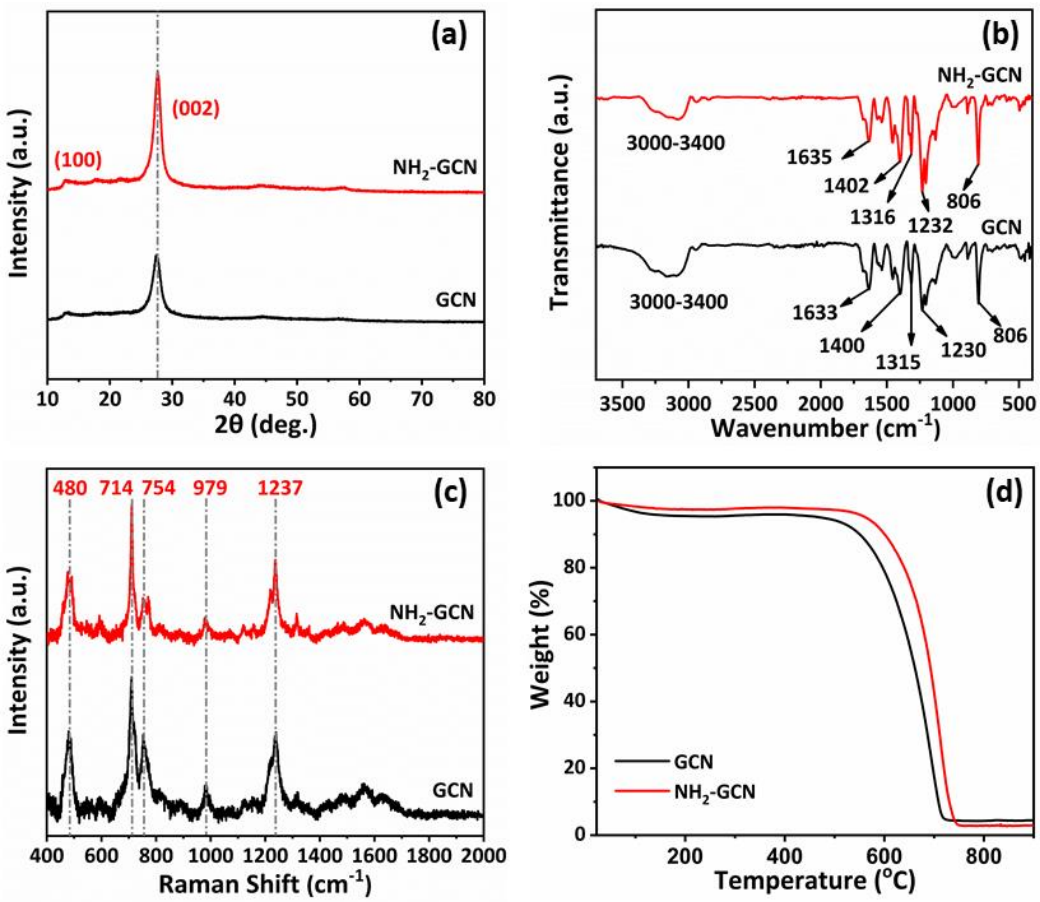

Figure 1. (a) PXRD pattern, (b) FTIR spectra, (c) Raman spectra and (d) TGA plot of GCN and NH_2-GCN nanosheets.

Thermal stability of the catalyst was examined using TGA, as shown in Figure 1 (d) and it was observed that the thermal stability of GCN was less than that of NH_2-GCN, due to its surface functionalization.[23] A weight loss of 4.6 % was observed for GCN up to 450 °C and for NH_2-GCN it was about 2.4 % up to 450 °C. This weight loss, up to 160 °C, is due to the absorbed water molecules in the nanosheets. This loss is less in the case of NH_2-GCN due to less absorption of water molecules because of increased hydrophobicity.[23, 39] The second weight loss observed between 200 – 400 °C for NH_2-GCN is very less whereas, in the case of GCN, the

second weight loss is more due to disintegration of -NH_2 group. Furthermore, in the range of 450 – 650 °C, complete decomposition of the C-N network of the heptazine ring occurs in both, GCN and NH_2-GCN. This is because the hydrogen bonding in both GCN and NH_2-GCN is not so strong as can tolerate that high temperature. Hence it gets completely disintegrated after 650 °C.[40]

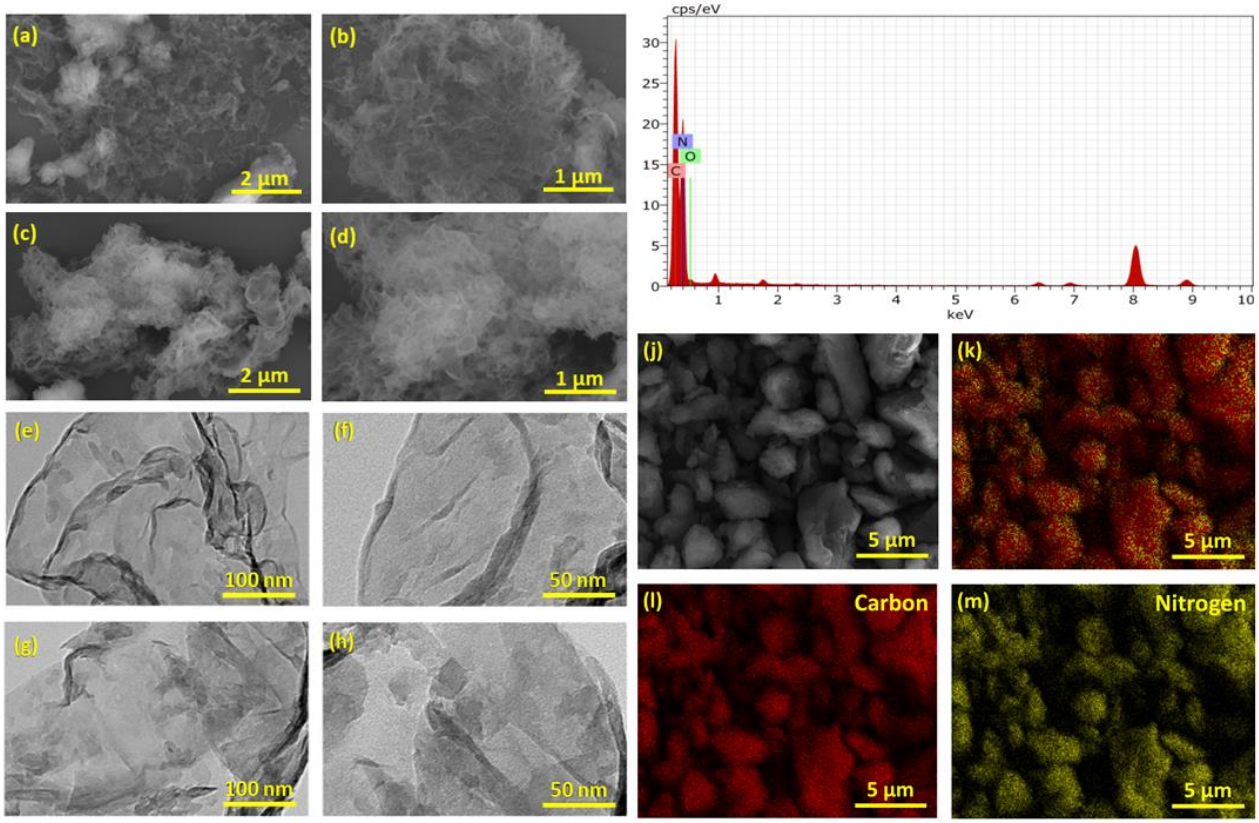

Figure 2. SEM images of (a, b) GCN and (c, d) NH_2-GCN, TEM images of (e, f) GCN and (g, h) NH_2-GCN, (i) EDAX analysis of NH_2-GCN, (j-m) EDX mapping images of NH_2-GCN nanosheets.

Morphology of GCN and NH_2-GCN were analyzed using SEM (as shown in Figure 2). The SEM images of GCN show crumbled and wavy sheet-like morphology. The SEM images of NH_2-GCN also showed crumbled sheet-like morphology where the nanosheets were stacked upon each other. The nanoscale morphologies were examined using TEM, which again showed sheet-like morphology in both GCN and NH_2-GCN. The sheets are present in compact form, wherein the sheets were agglomerated to form a non-uniform network which can be attributed to H-bonding and π-π stacking interactions between the layers.[41] The EDAX spectrum in (Figure 2i) and elemental mapping (Figure 2j-m) shows the presence of all constituent elements in the catalyst. The EDAX analysis (Figure S1, supporting information) from SEM also shows the

increase in the nitrogen content in NH_2-GCN nanosheets as compared to bare GCN. The nitrogen content is almost doubled upon amine-functionalization of GCN which confirmed the successful functionalization of GCN nanosheets.

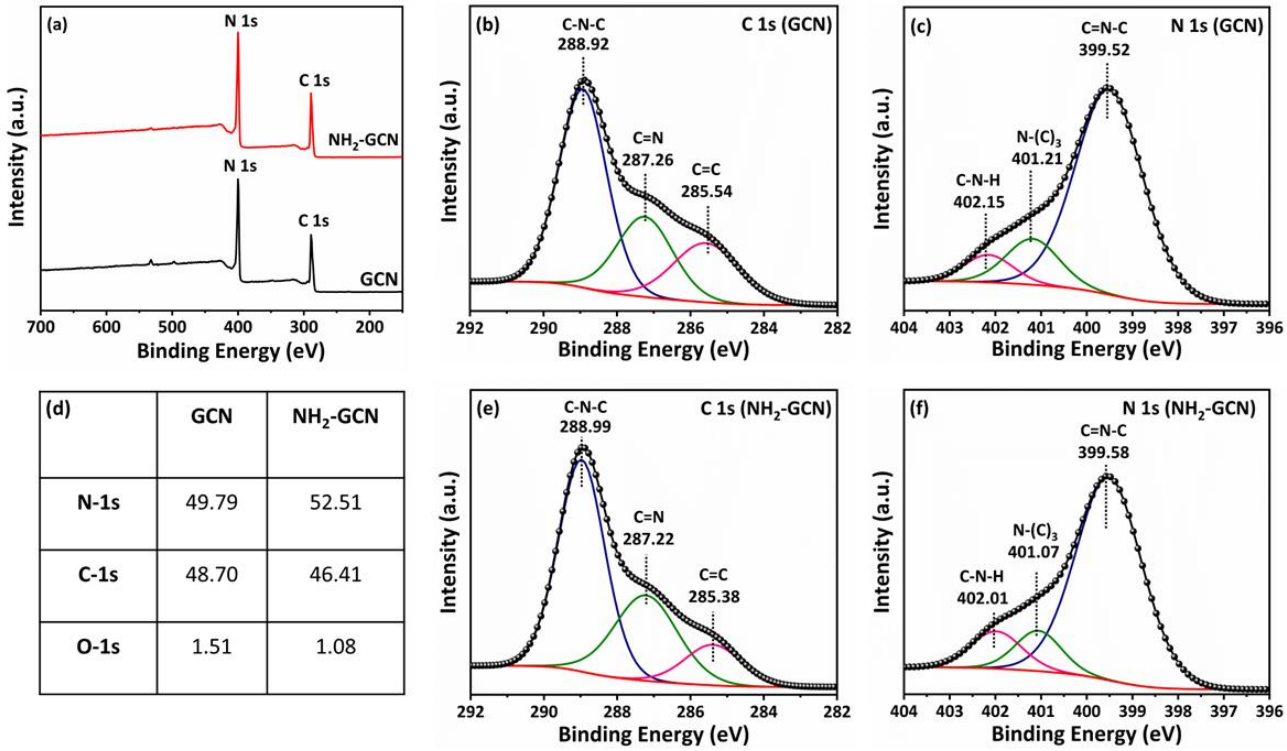

(d)	GCN	NH_2-GCN
N-1s	49.79	52.51
C-1s	48.70	46.41
O-1s	1.51	1.08

Figure 3. (a) Survey spectra of GCN and NH2-GCN nanosheets, XPS spectra (b) C 1s of GCN, (c) N 1s of GCN, (d) atomic composition of constitute elements in GCN and NH_2-GCN (e) C 1s of NH_2-GCN, and (f) N 1s of NH_2-GCN.

The compositional analysis of GCN and NH_2-GCN catalysts show the presence of carbon and nitrogen elements in the materials as depicted in the survey spectra (Figure 3a). It also represents the atomic percentage of all the constituent elements which show the increase in the N content of NH_2-GCN i.e., 49.79% in GCN and 52.51% in NH_2-GCN (Figure 3d). XPS spectrum of C 1s GCN, Figure 3(b), shows three major peaks at 288.92 eV, 287.26 eV, and 285.54 eV. The highest intensity peak of 288.92 eV corresponds to the sp^2 hybridized C-N bonds of the s-triazine unit. The relatively less intense peak at 287.26 eV is due to C=N bonds. The least intense peak at 285.54 eV can be attributed to the C=C bond of the trigonal C-N network. Figure 3(c) shows N 1s XPS spectra where the most intense peak at 399.52 eV corresponds to sp^2 hybridized N-atom bonded to carbon atoms in the s-triazine ring. The less

intense peaks at 401.21 eV and 402.15 eV corresponds to bridging N atoms in $(C)_3$ moieties and the C-N-H bond respectively.[42] The N 1s spectra of NH_2-GCN also shows similar peaks as GCN as same functional group (i.e., $-NH_2$) is present in both GCN and NH_2-GCN. However, the peaks in the C 1s and N 1s spectra of NH_2-GCN (Figure 3e, 3f respectively) are slightly shifted as compared to GCN due to the incorporation of various $-NH_2$ moieties.[35, 43]

Surface area and pore size distribution of GCN and NH_2-GCN was analyzed using BET (as shown in Figure S2, Supporting information). The liquid nitrogen adsorption-desorption isotherms of GCN and NH_2-GCN represents type IV physisorption and H3-hysteresis loops which shows the presence of mesopores and slit-like pores.[44] The surface area of GCN and NH_2-GCN nanosheets were found to be 55.444 $m^2\ g^{-1}$ and 22.548 $m^2\ g^{-1}$ respectively. Due to amine functionalization, the hydrogen bonding interactions in the NH_2-GCN layers are increased and the sheets get agglomerated which results in a lower surface area of NH_2-GCN as compared to GCN. The surface area and pore size distribution plots are also shown Figure S2 b-c and e-f. The mean pore size of GCN and NH_2-GCN was found to be 25.89 nm and 10.48 nm, as well as the mean pore volume, was estimated at 0.7178 $cm^3\ g^{-1}$ and 0.1182 $cm^3\ g^{-1}$ respectively.

By using TPD (Temperature Programmed Desorption), the surface composition of GCN and NH_2-GCN was measured. It measures the number of desorbed molecules of NH_3 and CO_2 probes from the surface of catalyst with increase in the temperature. The number of basic sites was measured by using CO_2 probe, because of the acidic nature of carbon dioxide it gets adsorbed on the basic sites present in the catalyst. NH_3 probe were used to determine the number of acidic sites present on the molecule due to its basic nature. The increase in the basic sites of NH_2-GCN was confirmed with the help of CO_2-TPD and the obtained plots are presented in (Figure S3, supporting information). The CO_2-TPD analysis showed that the total basic sites present in GCN were 0.043 mmol g^{-1} whereas in NH_2-GCN it was found to be 0.076 mmol g^{-1}. It showed that upon functionalization, the basic sites were almost doubled in NH_2-GCN due to the incorporation of more $-NH_2$ groups onto the surface of the nanosheets. The NH_3-TPD analysis showed that the total acidic sites present in NH_2-GCN were 0.069 mmol g^{-1} which are almost same as present in GCN (i.e., 0.071 mmol g^{-1}) which signifies that there is no change in the acidity of the catalyst. This confirms the successful functionalization of the catalyst.

4. CATALYTIC POTENTIAL

The catalytic ability of as-synthesized NH_2-GCN was tested for Knoevenagel condensation reactions. In this study, our main goal was to perform the reaction with a minimal amount of catalyst at an ambient temperature in environmentally benign solvent. So, to investigate the catalytic potential reaction conditions were optimized by varying several reaction parameters such as reaction time, temperature, catalytic amount, and solvent system. The model reaction was conducted using 4-nitrobenzaldehyde (1 mmol) and malononitrile (1 mmol) using 20 mg of NH_2-GCN catalyst and ethanol (3 mL) to obtain 2-(4-nitrobenzylidene) malononitrile at 25 ^{o}C. The product obtained was refined through column chromatography and was characterized using ^{1}H and ^{13}C NMR spectroscopic techniques.

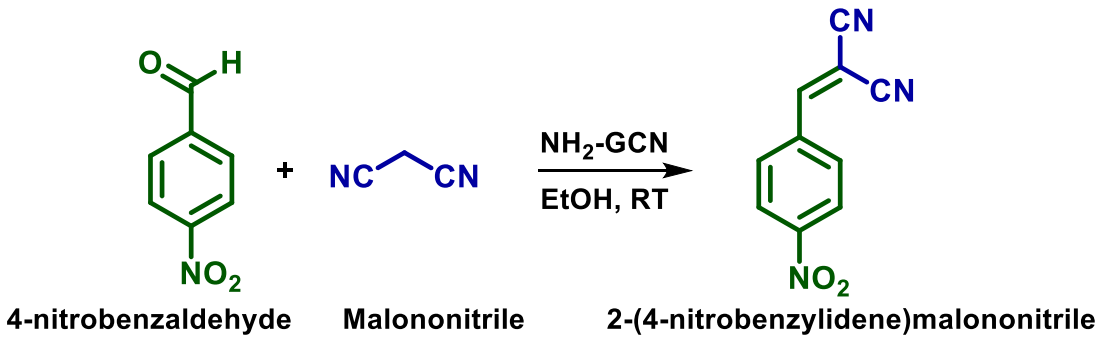

Scheme 2. Knoevenagel condensation reaction catalyzed by NH_2-GCN.

Various optimizations of reaction were carried out by using 4-nitrobenzaldehyde (1 mmol) and malononitrile (1 mmol) as a substrate. Firstly, the reaction was performed at room temperature to investigate the yield of the reaction by varying the amount of catalyst (entries 1-4). It was observed that major of the reactants were converted into products using 20 mg of the catalyst with the highest yield of 92%. When the amount of catalyst was 30 mg, the yield was 89%. So, we can say that 20 mg catalyst was an appropriate amount to carry out the reaction. The impact of reaction time was also studied. The amount of catalyst was taken at 20 mg and the temperature was constrained to be 25 ^{o}C. A relatively high yield of 81% was observed within 15 min. The yield increased from 81% to 92% within the next 45 min. Then after increasing the reaction time (entries 5-9) the yield decreased to 87%. Therefore 20 mg of catalyst and 60 min were the best-fitted catalyst amount and time respectively. In addition, the effect of temperature was also studied. Firstly, the reaction was conducted at room temperature (25 ^{o}C) using 20 mg of catalyst for 60 min. The highest yield of 92% was observed.

Further increasing the temperature, decreased the yield from 92% to 86% (entries 10-12). The effect of the solvent system was also studied for Knoevenagel condensation. Ethanol was chosen as a green solvent due to its less toxicity and environmentally friendly nature. Also, it gave a higher yield (entry 2) as compared to methanol, 2-propanol, and water (entries 13-15). Thus, the optimal condition for Knoevenagel condensation was estimated to be 1 mmol of 4-nitrobenzaldehyde, 1 mmol of malononitrile, 3 mL of ethanol, 20 mg NH_2-GCN catalyst, a reaction time of 60 min, and reaction temperature of 25 °C. Hence it is concluded that NH_2-GCN can effectively catalyze Knoevenagel condensation.

Table 1. Optimization of Knoevenagel condensation reaction[a] catalyzed by NH_2-GCN

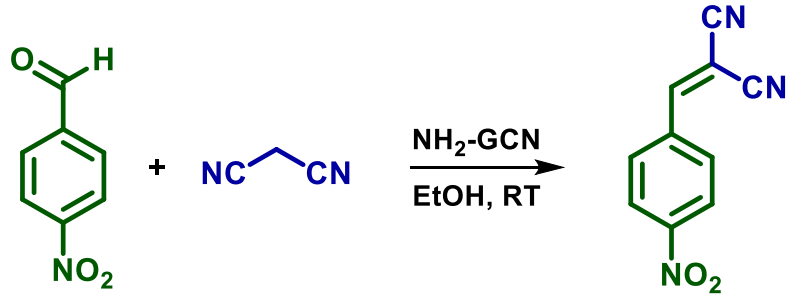

4-nitrobenzaldehyde **Malononitrile** **2-(4-nitrobenzylidene)malononitrile**

Entry	Catalyst (wt.)	Solvent	Temperature (°C)	Time (min)	Yield[b] (%)
1.	NH_2-GCN (10 mg)	EtOH	RT	60	67
2.	NH_2-GCN (20 mg)	EtOH	RT	60	92
3.	NH_2-GCN (30 mg)	EtOH	RT	60	89
4.	NH_2-GCN (20 mg)	EtOH	RT	15	81
5.	NH_2-GCN (20 mg)	EtOH	RT	30	85
6.	NH_2-GCN (20 mg)	EtOH	RT	45	87
7.	NH_2-GCN (20 mg)	EtOH	RT	90	86

8.	NH_2-GCN (20 mg)	EtOH	RT	120	87
9.	NH_2-GCN (20 mg)	EtOH	35	60	90
10.	NH_2-GCN (20 mg)	EtOH	45	60	91
11.	NH_2-GCN (20 mg)	EtOH	50	60	86
12.	NH_2-GCN (20 mg)	H_2O	RT	60	73
13.	NH_2-GCN (20 mg)	MeOH	RT	60	91
14.	NH_2-GCN (20 mg)	2-propanol	RT	60	86
[a] Reaction conditions: Carbonyl compound (1 mmol), active methylene compound (1 mmol), EtOH (3 mL), NH_2-GCN (20 mg). [b] Isolated yields.					

To study the role of steric hindrance and substituents on the catalytic potential of NH_2-GCN for Knoevenagel condensation, different types of aldehyde derivatives were used as substrates. All the reactions were performed under optimal conditions, as determined. The yields of corresponding products obtained varied from 79-92% (Table 2). Aldehydes with strong electron withdrawing substituents such as cyano, nitro, etc. showed the best efficiency which is due to the increased electrophilic nature of the substrates. And the aldehydes containing electron-donating groups showed a decrease in the yield which is due to the decrease in the electrophilicity of the carbonyl carbon. Also, the effect of substituents in ortho and meta position was studied. And it was found that the yield obtained is less as compared to the para position. The turnover number (TON) related to each reaction was calculated and its details are mentioned in S4 (Supporting information).

Table 2. Substrate scope of Knoevenagel condensation reaction[a] catalyzed by NH_2-GCN.

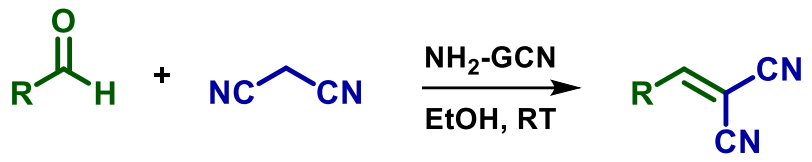

1a-1j 2a-2j 3a-3j

Entry	Carbonyl compound	Product	Time (min)	Yield[b] (%)	TON
1.	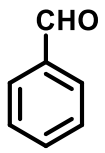	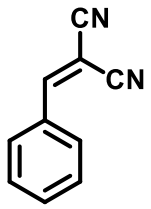	60	71	4896
2.	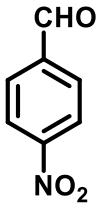	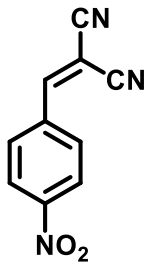	60	92	6345
3.	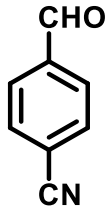	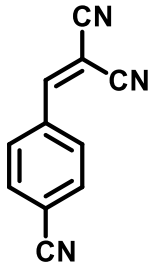	60	81	5586
4.	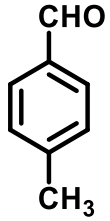	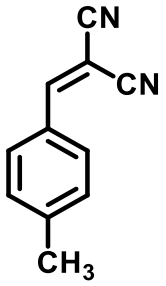	60	52	3586

5.	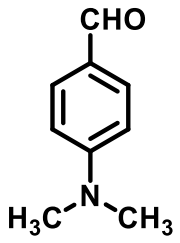	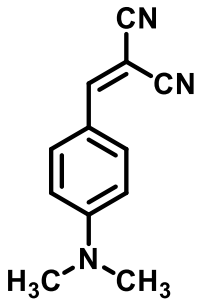	60	48	3310
6.	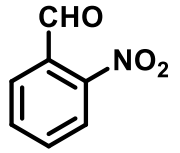	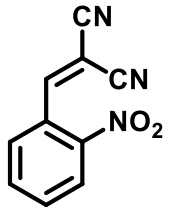	60	75	5172
7.	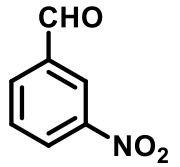	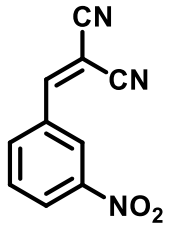	60	86	5931
8.	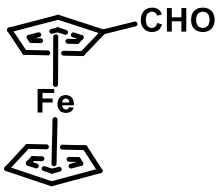	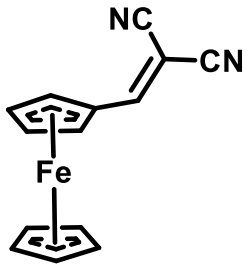	60	87	6000
9.	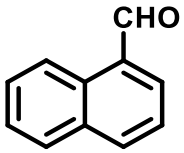	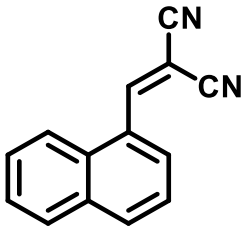	60	83	5724

10.	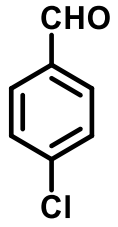	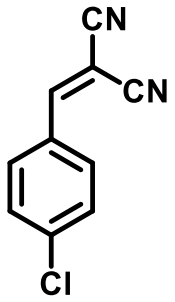	60	60	4138
11.	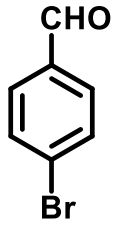	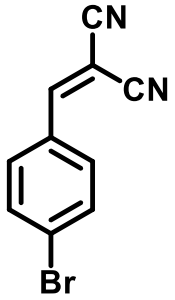	60	58	4000

[a] Reaction conditions: Carbonyl compound (1 mmol), active methylene compound (1 mmol), EtOH (3 mL), NH_2-GCN (20 mg). [b] Isolated yields.

In addition to that, the green metrics parameters were also studied to check the sustainability and environmental impact of the reaction as shown in Table 3. The detailed explanation of green metrics parameters is given in the S4 (supporting information).

Table 3. Summary of green metrics parameters calculated for the Knoevenagel condensation.

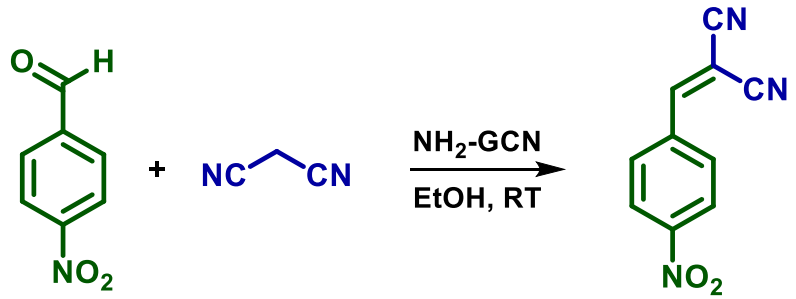

4-nitrobenzaldehyde Malononitrile 2-(4-nitrobenzylidene)malononitrile

Sl. No.	Green metrics parameters	Calculated values
1.	Environmental factor (E-factor)	0.16
2.	Atom economy (AE)	91.7 %

3.	Mass intensity (MI)	1.29
4.	Process mass intensity (PMI)	1.31
5.	Reaction mass efficiency (RME)	84.5 %

4.1 Plausible mechanism

A plausible mechanism for Knoevenagel condensation catalyzed by NH_2-GCN is presented in Scheme 3. At the beginning of the reaction, the basic sites of NH_2-GCN activates the carbonyl group of aldehydes via coordination (i), which accelerates the condensation step. The activated carbonyl carbon acts as an electrophilic center for the attack of the nucleophile. Afterward, the proton from the active methylene moiety of malononitrile gets abstracted by NH_2-GCN which makes it nucleophilic in nature. Which then attacks the electrophilic center of carbonyl carbon (ii) to form intermediate (iii). Further dehydration occurs to form a C=C bond resulting in the Knoevenagel product. This mechanism can explain the catalytic efficiency of NH_2-GCN when different aldehyde substrates were varied for Knoevenagel condensation. Aldehydes having strong electron withdrawing substituents such as cyano, nitro, etc. showed the best efficiency which is due to the increased electrophilic nature of the substrates and makes the nucleophilic attack easier. And the aldehydes containing electron-donating groups showed less yield which is due to the decrease in the electrophilicity of the carbonyl carbon. So, this mechanism nicely explains the effect of substituents on the catalytic behavior of NH_2-GCN catalyst.

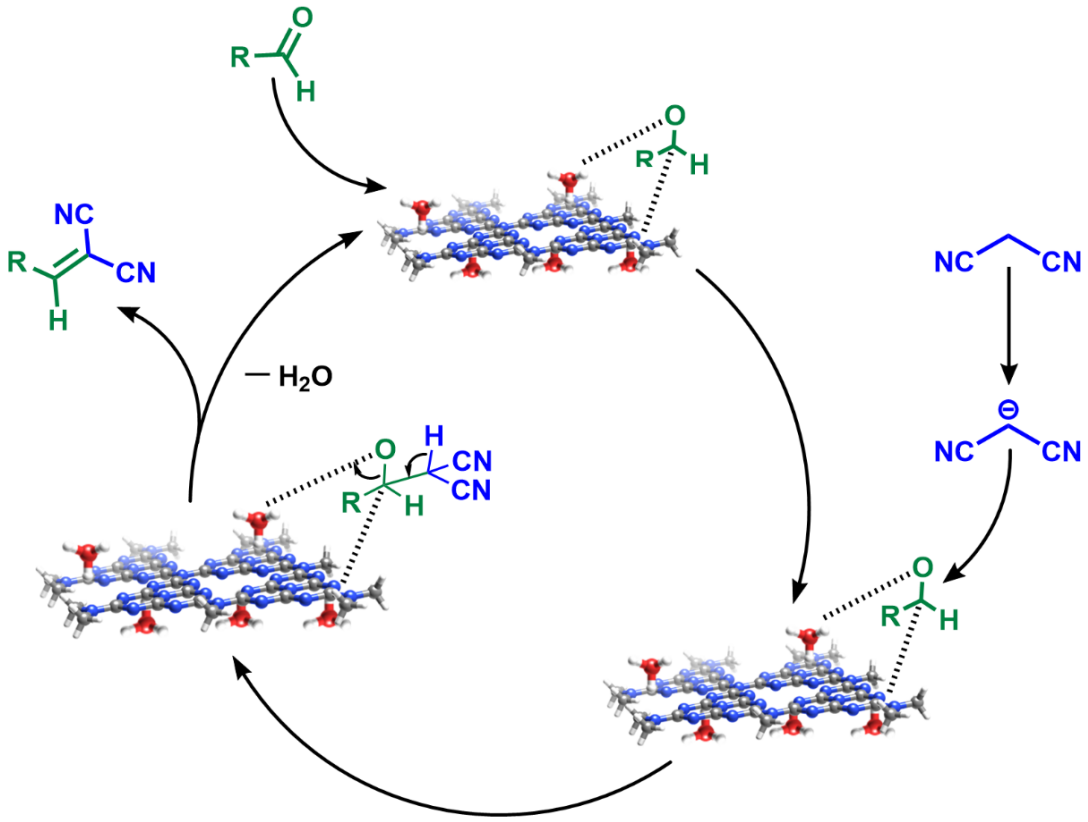

Scheme 3. Plausible mechanism for Knoevenagel condensation reaction catalyzed by NH_2-GCN.

5. RECYCLABILITY

Reusability and recyclability of catalyst are important criteria to examine the heterogeneous nature of the catalyst. In this context, the recyclability studies were carried out for Knoevenagel condensation under the pre-determined optimal reaction conditions using 4-nitrobenzaldehyde (5 mmol), malononitrile (5 mmol), ethanol (15 mL), and 100 mg of NH_2-GCN catalyst as shown in Figure 4 (a). The catalyst was then recovered by centrifugation and further washed with DI water and ethanol multiple times. Then the catalyst was then dried in the oven at 80 ^{o}C overnight and further used for the next cycle. After each cycle, the yield of the reaction was calculated. Only a slight decrease in the yield of the reaction was observed, which was due to the loss of catalyst. The yield decreased from 92 % to 83 % after the 5th cycle. Then PXRD measurements (Figure 4 (b)) were performed for the recovered catalyst

after 5 cycles to examine the stability of the catalyst. The recovered and fresh catalyst shows almost similar peaks which demonstrates the stability of the as-synthesized catalysts.

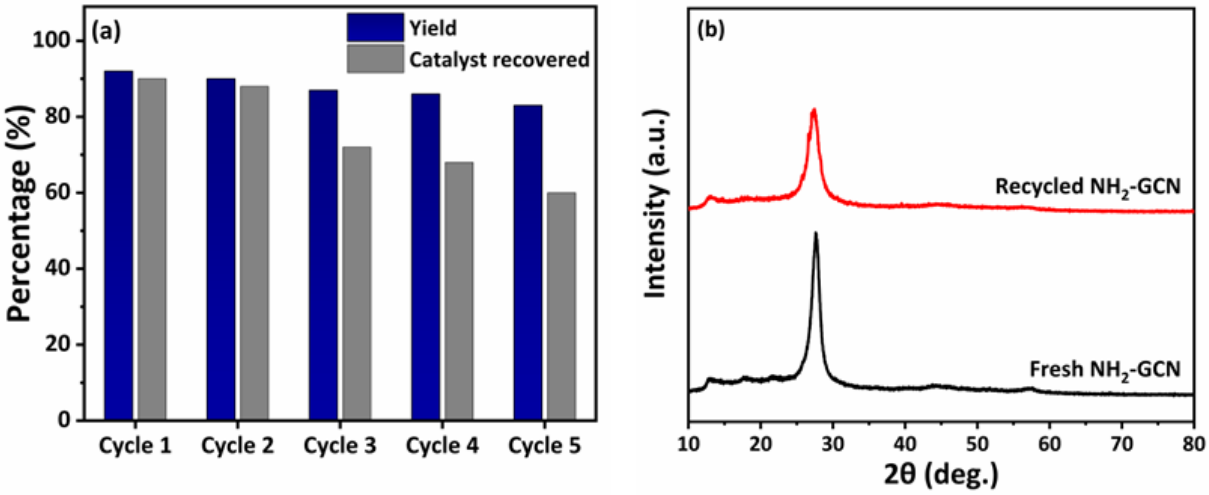

Figure 4. (a) Recyclability study of NH_2-GCN for Knoevenagel condensation, (b) PXRD pattern of fresh and recycled catalyst.

6. CONCLUSION

Finally, it may be concluded that a catalytic system of high efficiency and sustainability was developed for Knoevenagel condensation by surface functionalization of GCN with the amine groups. The structural analysis of synthesized GCN and NH_2-GCN was successfully conducted through XRD, FTIR, Raman spectroscopy, and TPD analysis. The morphological studies of obtained GCN and NH_2-GCN were investigated through SEM and TEM and the compositional analysis was done by XPS. The surface functionalization resulted in increased basicity of the catalyst, leading to its higher stability and better catalytic activity for the Knoevenagel condensation reaction with high yield and TON values. The reactions were performed by using minimal amount of catalyst at an ambient temperature in environmentally benign solvent. The reactions were carried out in lesser reaction time due to the increased electrophilicity of the substrates. Also, the recyclability studied reveals the good stability of the catalyst and it can be used after 5 cycles without showing much decrease in the yield. This study provides a relatively novel and green approach to the Knoevenagel condensation reaction.

ACKNOWLEDGEMENTS

The authors thank Advanced Materials Research Centre (AMRC), IIT Mandi, for laboratory and characterization facilities. Devendra Sharma acknowledges the doctoral scholarship from the Ministry of Education (MoE), India.

CONFLICT OF INTEREST

Authors declare no conflict of interest.

REFERENCES

(1) Kumar, A.; Choudhary, P.; Krishnan, V. Selective and efficient aerobic oxidation of benzyl alcohols using plasmonic Au-TiO2: Influence of phase transformation on photocatalytic activity. *Applied Surface Science* **2022**, *578*, 151953.

(2) Wang, S.-S.; Zhang, Q.-L.; Chu, P.; Kong, L.-Q.; Li, G.-Z.; Li, Y.-Q.; Yang, L.; Zhao, W.-J.; Guo, X.-H.; Tang, Z.-Y. Synthesis and antitumor activity of α, β-unsaturated carbonyl moiety-containing oleanolic acid derivatives targeting PI3K/AKT/mTOR signaling pathway. *Bioorganic Chemistry* **2020**, *101*, 104036.

(3) Verochkina, E. A.; Vchislo, N. V.; Rozentsveig, I. B. α-functionally substituted α, β-unsaturated aldehydes as fine chemicals reagents: Synthesis and application. *Molecules* **2021**, *26* (14), 4297.

(4) Li, G.; Xiao, J.; Zhang, W. Efficient and reusable amine-functionalized polyacrylonitrile fiber catalysts for Knoevenagel condensation in water. *Green Chemistry* **2012**, *14* (8), 2234-2242. áJustin Thomas, K. Rose bengal photocatalyzed Knoevenagel condensation of aldehydes and ketones in aqueous medium. *Green Chemistry* **2022**, *24* (12), 4952-4957.

(5) Hangarge, R. V.; Jarikote, D. V.; Shingare, M. S. Knoevenagel condensation reactions in an ionic liquid. *Green Chemistry* **2002**, *4* (3), 266-268.

(6) van Schijndel, J.; Molendijk, D.; Spakman, H.; Knaven, E.; Canalle, L. A.; Meuldijk, J. Mechanistic considerations and characterization of ammonia-based catalytic active intermediates of the green Knoevenagel reaction of various benzaldehydes. *Green Chemistry Letters and Reviews* **2019**, *12* (3), 323-331.

(7) Burate, P. A.; Javle, B. R.; Desale, P. H.; Kinage, A. K. Amino acid amide based ionic liquid as an efficient organo-catalyst for solvent-free Knoevenagel condensation at room temperature. *Catalysis Letters* **2019**, *149* (9), 2368-2375.

(8) Hiba, K.; Prathapan, S.; Sreekumar, K. Amine Functionalized Dendronized Polymer as a Homogeneous Base Catalyst for the Synthesis of Polyhydroquinolines and 4-Arylidene-3-Methylisoxazol-5 (4H)-Ones. *Catalysis Letters* **2021**, 1-13.

(9) Kumar, A.; Choudhary, P.; Kumar, A.; Camargo, P. H.; Krishnan, V. Recent advances in plasmonic photocatalysis based on TiO2 and noble metal nanoparticles for energy conversion, environmental remediation, and organic synthesis. *Small* **2022**, *18* (1), 2101638.

(10) Li, P.; Cao, C.-Y.; Chen, Z.; Liu, H.; Yu, Y.; Song, W.-G. Core–shell structured mesoporous silica as acid–base bifunctional catalyst with designated diffusion path for cascade reaction sequences. *Chemical communications* **2012**, *48* (85), 10541-10543.

(11) Low, J.; Cao, S.; Yu, J.; Wageh, S. Two-dimensional layered composite photocatalysts. *Chemical communications* **2014**, *50* (74), 10768-10777. Wang, X.; Blechert, S.; Antonietti, M. Polymeric graphitic carbon nitride for heterogeneous photocatalysis. *Acs Catalysis* **2012**, *2* (8), 1596-1606.

(12) Min, H.-K.; An, H.; Kang, D.-C.; Kweon, S.; Baek, S.-H.; Park, M. B.; Shin, C.-H. Rational Design of Pomegranate-like Base–Acid Bifunctional β Zeolite by Steam-Assisted Crystallization for the Tandem Deacetalization–Knoevenagel Condensation. *ACS Applied Materials & Interfaces* **2020**, *12* (52), 57881-57887.

(13) Devi, R.; Begum, P.; Bharali, P.; Deka, R. C. Comparative study of potassium salt-loaded MgAl hydrotalcites for the Knoevenagel condensation reaction. *ACS omega* **2018**, *3* (6), 7086-7095.

(14) Cai, K.; Tan, W.; Zhao, N.; He, H. Design and assembly of a hierarchically micro-and mesoporous MOF as a highly efficient heterogeneous catalyst for Knoevenagel condensation reaction. *Crystal Growth & Design* **2020**, *20* (7), 4845-4851. Zhao, Z.-S.; Zhang, Y.; Fang, T.; Han, Z.-B.; Liang, F.-S. Chitosan-Coated Metal–Organic-Framework Nanoparticles as Catalysts for Tandem Deacetalization–Knoevenagel Condensation Reactions. *ACS Applied Nano Materials* **2020**, *3* (7), 6316-6320.

(15) Jiang, L.; Shi, X.-L.; Lv, Y.; Gong, H.; Liu, S.; Du, M.; Hu, Q.; Shi, K. Acid-base bifunctional catalysis by a heteropolyacid and amines on the polyetheretherketone fiber for cleaner acceleration of the one-pot tandem reactions. *Journal of Industrial and Engineering Chemistry* **2022**.

(16) **!!! INVALID CITATION !!! 16**.

(17) Cai, M.; Wang, X.; Fang, Y.; Chen, Y.; Dai, L. Robust Mg (Ca) Zr-Doped Acid–Base Bifunctional Mesoporous Silica and Their Applications in the Deacetalization-Knoevenagel Reaction. *Inorganic Chemistry* **2021**, *60* (12), 8924-8935. Kumar, Y.; Shabir, J.; Gupta, P.; Kumar, L. S. Design and development of amine functionalized mesoporous cubic silica particles: a recyclable catalyst for knoevenagel condensation. *Catalysis Letters* **2022**, *152* (5), 1506-1516.

(18) Choudhary, P.; Bahuguna, A.; Kumar, A.; Dhankhar, S. S.; Nagaraja, C.; Krishnan, V. Oxidized graphitic carbon nitride as a sustainable metal-free catalyst for hydrogen transfer reactions under mild conditions. *Green Chemistry* **2020**, *22* (15), 5084-5095.

(19) Han, C.; Meng, P.; Waclawik, E. R.; Zhang, C.; Li, X. H.; Yang, H.; Antonietti, M.; Xu, J. Palladium/Graphitic carbon nitride (g-C3N4) stabilized emulsion microreactor as a store for hydrogen from ammonia borane for use in alkene hydrogenation. *Angewandte Chemie International Edition* **2018**, *57* (45), 14857-14861. Altan, O.; Kalay, E. The influence of band bending phenomenon on photocatalytic Suzuki-Miyaura coupling reaction: The case of AgPd alloy nanoparticles supported on graphitic carbon nitride. *Applied Surface Science* **2022**, *580*, 152287.

(20) Zhu, J.; Xiao, P.; Li, H.; Carabineiro, S. A. Graphitic carbon nitride: synthesis, properties, and applications in catalysis. *ACS applied materials & interfaces* **2014**, *6* (19), 16449-16465.

(21) Choudhary, P.; Kumar, A.; Krishnan, V. Nanoarchitectonics of phosphorylated graphitic carbon nitride for sustainable, selective and metal-free synthesis of primary amides. *Chemical Engineering Journal* **2022**, *431*, 133695.

(22) Li, H.; Wang, L.; Liu, Y.; Lei, J.; Zhang, J. Mesoporous graphitic carbon nitride materials: synthesis and modifications. *Research on Chemical Intermediates* **2016**, *42* (5), 3979-3998.

(23) Sierra, U.; Cuara, E.; Mercado, A.; Díaz-Barriga, E.; Bahena, A.; Cortés, A.; Martínez, J. P.; Solà, M.; Fernández, S. Efficient synthesis of amine-functionalized graphene oxide by ultrasound-assisted reactions and density functional theory mechanistic insight. *Applied Nanoscience* **2021**, *11* (5), 1637-1649.

(24) Xu, H.; Pan, L.; Fang, X.; Liu, B.; Zhang, W.; Lu, M.; Xu, Y.; Ding, T.; Chang, H. Knoevenagel condensation catalyzed by novel Nmm-based ionic liquids in water. *Tetrahedron Letters* **2017**, *58* (24), 2360-2365.

(25) Postole, G.; Chowdhury, B.; Karmakar, B.; Pinki, K.; Banerji, J.; Auroux, A. Knoevenagel condensation reaction over acid–base bifunctional nanocrystalline CexZr1− xO2 solid solutions. *Journal of Catalysis* **2010**, *269* (1), 110-121.

(26) Kalantari, F.; Rezayati, S.; Ramazani, A.; Aghahosseini, H.; Ślepokura, K.; Lis, T. Proline-Cu Complex Based 1, 3, 5-Triazine Coated on Fe3O4 Magnetic Nanoparticles: A Nanocatalyst for the Knoevenagel Condensation of Aldehyde with Malononitrile. *ACS Applied Nano Materials* **2022**, *5* (2), 1783-1797.

(27) Yue, C.; Mao, A.; Wei, Y.; Lü, M. Knoevenagel condensation reaction catalyzed by task-specific ionic liquid under solvent-free conditions. *Catalysis Communications* **2008**, *9* (7), 1571-1574.

(28) Rashidizadeh, A.; Esmaili Zand, H. R.; Ghafuri, H.; Rezazadeh, Z. Graphitic carbon nitride nanosheet/FeWO4 nanoparticle composite for tandem photooxidation/knoevenagel condensation. *ACS Applied Nano Materials* **2020**, *3* (7), 7057-7065.

(29) Kumar, L.; Verma, N.; Sehrawat, H.; Tomar, R.; Kumar, R.; Chandra, R. Successive oxidation–condensation reactions using a multifunctional gold-supported nanocomposite (Au/MgCe–HDO). *New Journal of Chemistry* **2022**, *46* (7), 3472-3481.

(30) Balalaie, S.; Nemati, N. Ammonium acetate-basic alumina catalyzed Knoevenagel condensation under microwave irradiation under solvent-free condition. *Synthetic Communications* **2000**, *30* (5), 869-875.

(31) Badiger, K. B.; Kamanna, K. Knoevenagel condensation reaction catalysed by agro-waste extract as a greener solvent catalyst. *Org Commun* **2021**, *14*, 81-91.

(32) Maleki, R.; Koukabi, N.; Kolvari, E. Fe3O4-Methylene diphenyl diisocyanate-guanidine (Fe3O4–4, 4'-MDI-Gn): A novel superparamagnetic powerful basic and recyclable nanocatalyst as an efficient heterogeneous catalyst for the Knoevenagel condensation and tandem Knoevenagel-Michael-cyclocondensation reactions. *Applied Organometallic Chemistry* **2018**, *32* (1), e3905.

(33) Pei, X.; Xiong, D.; Wang, H.; Gao, S.; Zhang, X.; Zhang, S.; Wang, J. Reversible phase transfer of carbon dots between an organic phase and aqueous solution triggered by CO2. *Angewandte Chemie* **2018**, *130* (14), 3749-3753.

(34) Fina, F.; Callear, S. K.; Carins, G. M.; Irvine, J. T. Structural investigation of graphitic carbon nitride via XRD and neutron diffraction. *Chemistry of Materials* **2015**, *27* (7), 2612-2618. Yadav, A.; Kang, S.-W.; Hunge, Y. Photocatalytic degradation of Rhodamine B using graphitic

carbon nitride photocatalyst. *Journal of Materials Science: Materials in Electronics* **2021**, *32* (11), 15577-15585. Liu, B.; Ye, L.; Wang, R.; Yang, J.; Zhang, Y.; Guan, R.; Tian, L.; Chen, X. Phosphorus-doped graphitic carbon nitride nanotubes with amino-rich surface for efficient CO2 capture, enhanced photocatalytic activity, and product selectivity. *ACS applied materials & interfaces* **2018**, *10* (4), 4001-4009.

(35) Li, F.; Zhou, H.; Fan, J.; Xiang, Q. Amine-functionalized graphitic carbon nitride decorated with small-sized Au nanoparticles for photocatalytic CO2 reduction. *Journal of colloid and interface science* **2020**, *570*, 11-19.

(36) Paul, D. R.; Sharma, R.; Nehra, S.; Sharma, A. Effect of calcination temperature, pH and catalyst loading on photodegradation efficiency of urea derived graphitic carbon nitride towards methylene blue dye solution. *RSC advances* **2019**, *9* (27), 15381-15391. Fard, M. A. D.; Ghafuri, H.; Rashidizadeh, A. Sulfonated highly ordered mesoporous graphitic carbon nitride as a super active heterogeneous solid acid catalyst for Biginelli reaction. *Microporous and Mesoporous Materials* **2019**, *274*, 83-93.

(37) Xu, J.; Zhang, L.; Shi, R.; Zhu, Y. Chemical exfoliation of graphitic carbon nitride for efficient heterogeneous photocatalysis. *Journal of Materials Chemistry A* **2013**, *1* (46), 14766-14772.

(38) Ibrahim, A.; Memon, U.; Duttagupta, S.; Mahesh, I.; Raman, R. S.; Sarkar, A.; Pendharkar, G.; Tatiparti, S. Nano-structured palladium impregnate graphitic carbon nitride composite for efficient hydrogen gas sensing. *International Journal of Hydrogen Energy* **2020**, *45* (17), 10623-10636.

(39) Hosseini, Y.; Najafi, M.; Khalili, S.; Jahanshahi, M.; Peyravi, M. Assembly of amine-functionalized graphene oxide for efficient and selective adsorption of CO2. *Materials Chemistry and Physics* **2021**, *270*, 124788. Fan, J.; Yang, J.; Wang, L.; Li, H.; Tian, J.; Ye, J.; Zhao, Y. Enhanced mechanical properties of epoxy nanocomposites with mildly surface-functionalized graphene oxide by tuned amine species. *Applied Surface Science* **2021**, *558*, 149964.

(40) Hajinasiri, R.; Ghafuri, H.; Hossaini, Z. Synthesis and characterization of graphitic carbon nitride supported Tris (hydroxymethyl) aminomethanes) g-C3N4/THAM) as a novel catalyst for the synthesis of poly hydroquinoline and pyranopyrazole derivatives. *Polyhedron* **2022**, *221*, 115878.

(41) Li, X.; Zhang, J.; Shen, L.; Ma, Y.; Lei, W.; Cui, Q.; Zou, G. Preparation and characterization of graphitic carbon nitride through pyrolysis of melamine. *Applied Physics A* **2009**, *94* (2), 387-392.

(42) Titantah, J.; Lamoen, D. Carbon and nitrogen 1s energy levels in amorphous carbon nitride systems: XPS interpretation using first-principles. *Diamond and related materials* **2007**, *16* (3), 581-588. Suter, T.; Brázdová, V.; McColl, K.; Miller, T. S.; Nagashima, H.; Salvadori, E.; Sella, A.; Howard, C. A.; Kay, C. W.; Corà, F. Synthesis, structure and electronic properties of graphitic carbon nitride films. *The Journal of Physical Chemistry C* **2018**, *122* (44), 25183-25194. Devi, M.; Barbhuiya, M. H.; Das, B.; Bhuyan, B.; Dhar, S. S. Modified mesoporous graphitic carbon nitride: a novel high-performance heterogeneous base catalyst for transesterification reaction. *Sustainable Energy & Fuels* **2020**, *4* (7), 3537-3545.

(43) Zhang, F.; Jiang, H.; Li, X.; Wu, X.; Li, H. Amine-functionalized GO as an active and reusable acid–base bifunctional catalyst for one-pot cascade reactions. *ACS Catalysis* **2014**, *4* (2), 394-401.

(44) Kumar, A.; Reddy, K. L.; Kumar, S.; Kumar, A.; Sharma, V.; Krishnan, V. Rational design and development of lanthanide-doped NaYF4@ CdS–Au–RGO as quaternary plasmonic photocatalysts for harnessing visible–near-infrared broadband spectrum. *ACS applied materials & interfaces* **2018**, *10* (18), 15565-15581. Rajkumar, C.; Veerakumar, P.; Chen, S.-M.; Thirumalraj, B.; Lin, K.-C. Ultrathin sulfur-doped graphitic carbon nitride nanosheets as metal-free catalyst for electrochemical sensing and catalytic removal of 4-nitrophenol. *ACS Sustainable Chemistry & Engineering* **2018**, *6* (12), 16021-16031. Kumar, A.; Choudhary, P.; Kumar, K.; Kumar, A.; Krishnan, V. Plasmon induced hot electron generation in two dimensional carbonaceous nanosheets decorated with Au nanostars: enhanced photocatalytic activity under visible light. *Materials Chemistry Frontiers* **2021**, *5* (3), 1448-1467.